YMTHE, Volume *30*

Supplemental Information

Targeting of pancreatic cancer cells and stromal cells using engineered oncolytic *Salmonella typhimurium*

Wenzhi Tan, Mai Thi-Quynh Duong, Chaohui Zuo, Yeshan Qin, Ying Zhang, Yanxia Guo, Yeongjin Hong, Jin Hai Zheng, and Jung-Joon Min

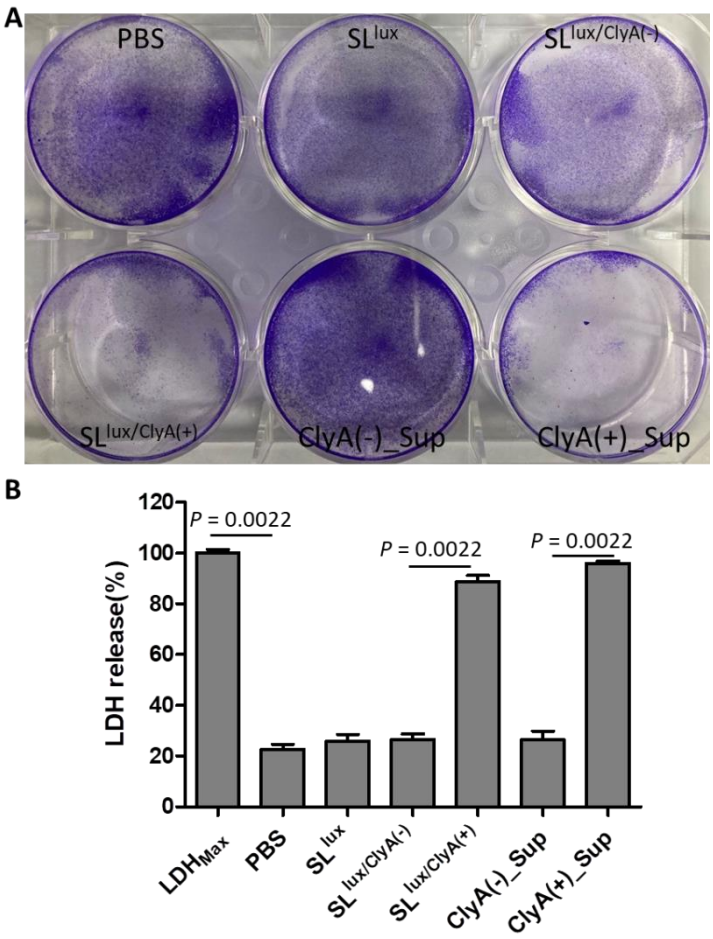

Figure S1. In vitro cell killing of AsPC-1 by ClyA-expressing bacteria. 1×10^6 cell/well were seeded in a 6-well plate, and after 24 h, the cells were co-cultured with 100 MOI (multiplicity of infection, bacteria: cell = 100:1) SL^{lux} and $SL^{lux/ClyA}$ with or without 8 h induction of 0.2% L-arabinose. 120 μg/ml of gentamycin was subsequently added into the culture, and the culture was maintained for another 36 h. Bacteria culture supernatant (Sup) collected from $SL^{lux/ClyA}$ with or without 8 h induction of 0.2% L-arabinose was also added to the cells as shown in the last two wells at a final concentration of 15% (v/v). (A) The plate was stained with crystal violet after 36 h treatment. (B) Lactate dehydrogenase (LDH) release was measured in the cell-culture supernatant. Completely lysed cells served as the positive control (LDH_{Max}, n = 6).

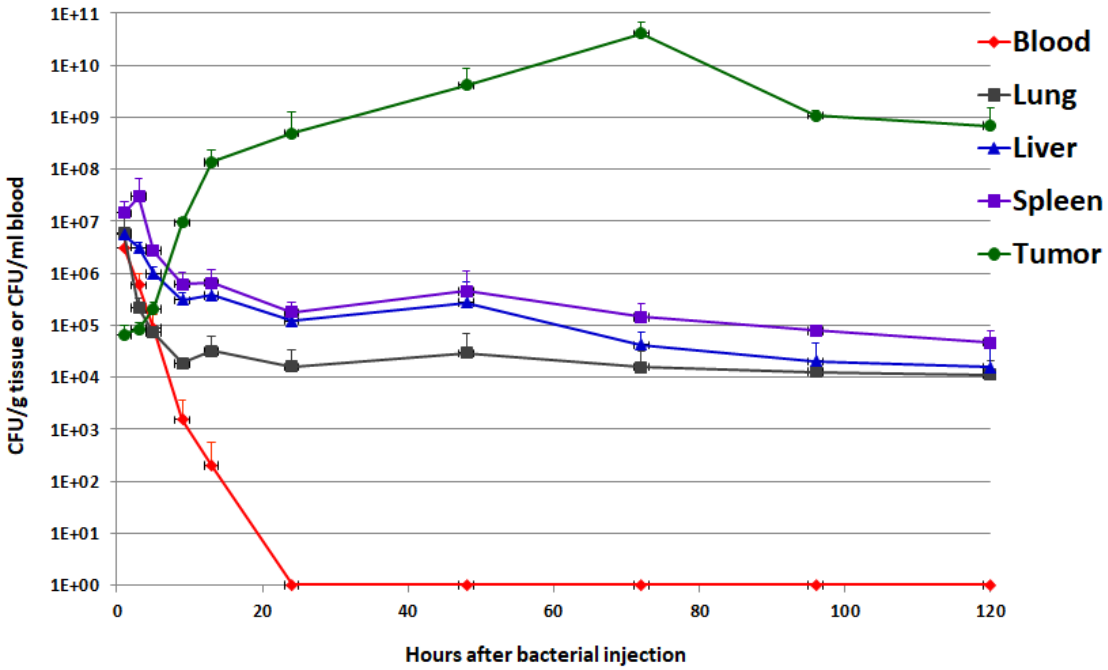

Figure S2. Bacterial biodistribution in vivo. Attenuated bacteria have broad and very specific targeting abilities toward various kinds of solid tumors, and the MC38 murine colon cancer in immunocompetent C57BL/6 mice was applied to. Samples were collected from MC38 tumor-bearing mice at indicated time points post-bacterial infection. Viable bacterial numbers were quantified with colony counts to study the biodistribution of attenuated *Salmonella typhimurium* (SL) in vivo (n = 11).

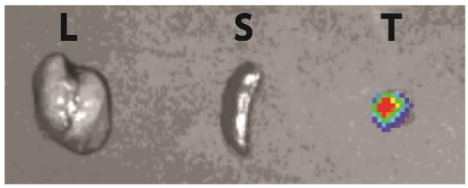

Figure S3. Ex vivo imaging of AsPC-1 xenografts post-bacterial injection. AsPC-1 (n = 11 mice per group) cancer model mice were treated with engineered $SL^{lux/ClyA}$. When the tumor reached 100–120 mm^3, mice were treated with 3.0×10^7 CFU engineered bacteria. Bacterial bioluminescence, as monitored by IVIS imaging, at 3 dpi. L: liver, S: spleen, T: tumor.

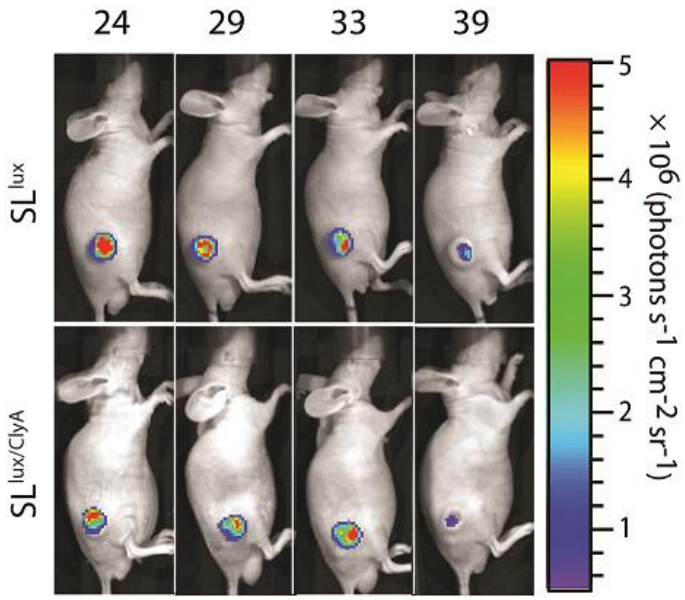

Figure S4. Bacterial colonization of AsPC-1 subcutaneous tumors. AsPC-1 (n = 12 mice per group) cancer model mice were treated with engineered *Salmonella*. When the tumors reached 100–120 mm^3, mice were treated with 3.0×10^7 CFU engineered SL^{lux} or $SL^{lux/ClyA}$. Bacterial bioluminescence, as monitored by IVIS imaging, in a representative mouse from each group.

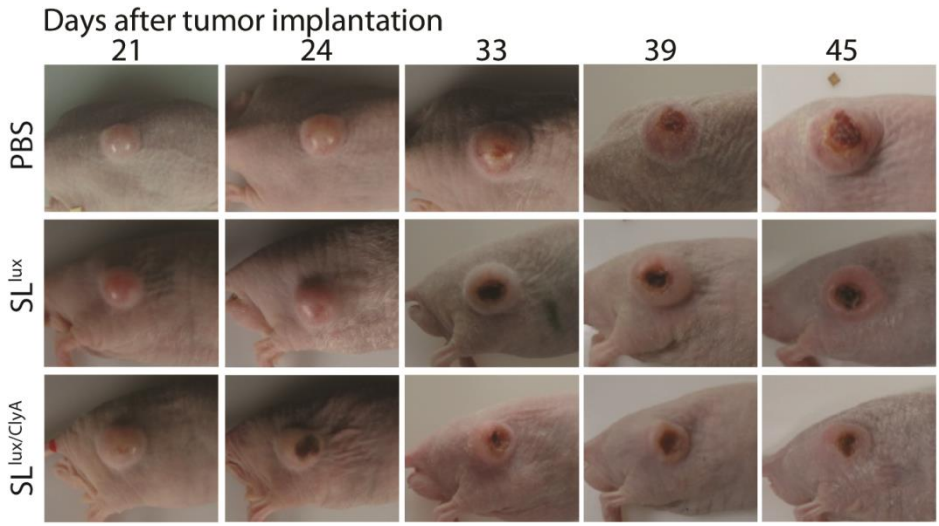

Figure S5. Photographs of representative AsPC-1 cancer model mice. AsPC-1 (n = 12 mice per group) cancer model mice were treated with PBS, engineered SL^{lux}, or $SL^{lux/ClyA}$. When the tumor reached 100–120 mm^3, mice were treated with 3.0×10^7 CFU engineered bacteria. Representative photos from each group are shown.

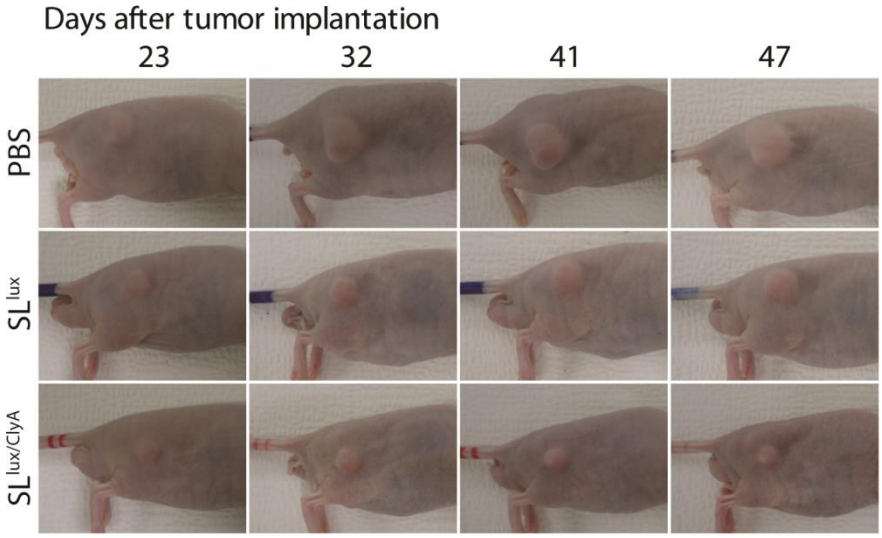

Figure S6. Photographs of representative Capan-2 cancer model mice. Capan-2 (n = 10 mice per group) cancer model mice were treated with PBS, engineered SL^{lux}, or $SL^{lux/ClyA}$. When the tumor reached 100–120 mm^3, mice were treated with 3.0×10^7 CFU engineered bacteria. Representative photos from each group are shown.

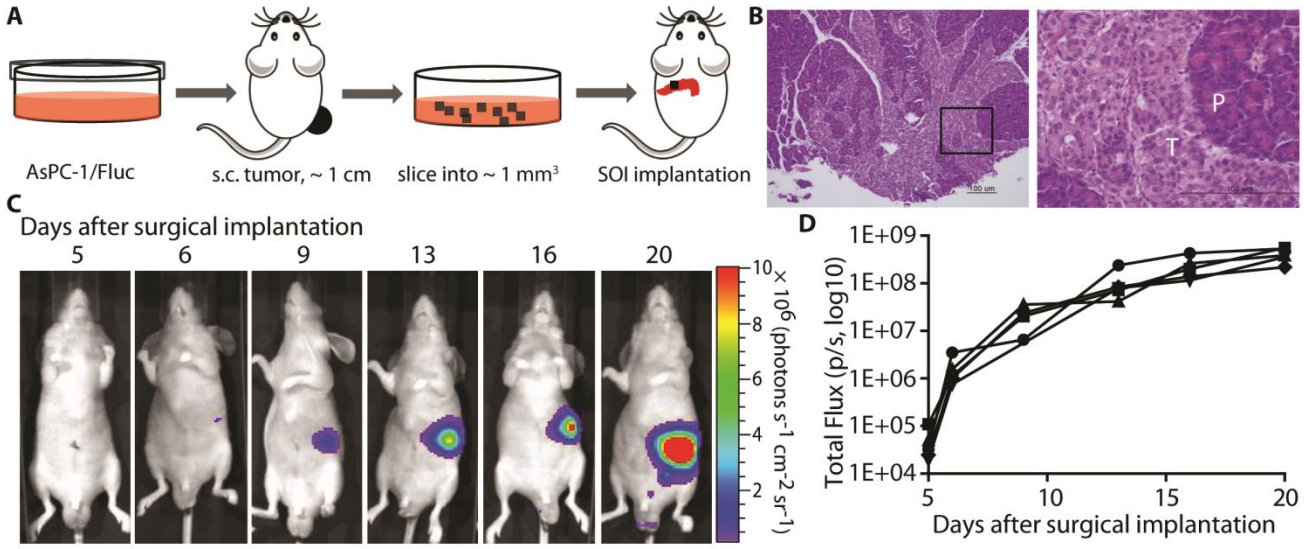

Figure S7. Generation of an orthotopic pancreatic cancer model in nude mice. (A) Schematic showing the generation of an orthotopic pancreatic cancer model. (B) Confirmation of local tumor invasion (Day 11) into normal pancreatic tissue (H&E staining; n = 6 mice). Scale bar = 100 μm. (C) Representative bioluminescence images showing developmental dynamics of orthotopic pancreatic cancer (AsPC-1/Fluc), as monitored by IVIS. (D) Changes in tumor total Flux in individual mouse (n = 5).

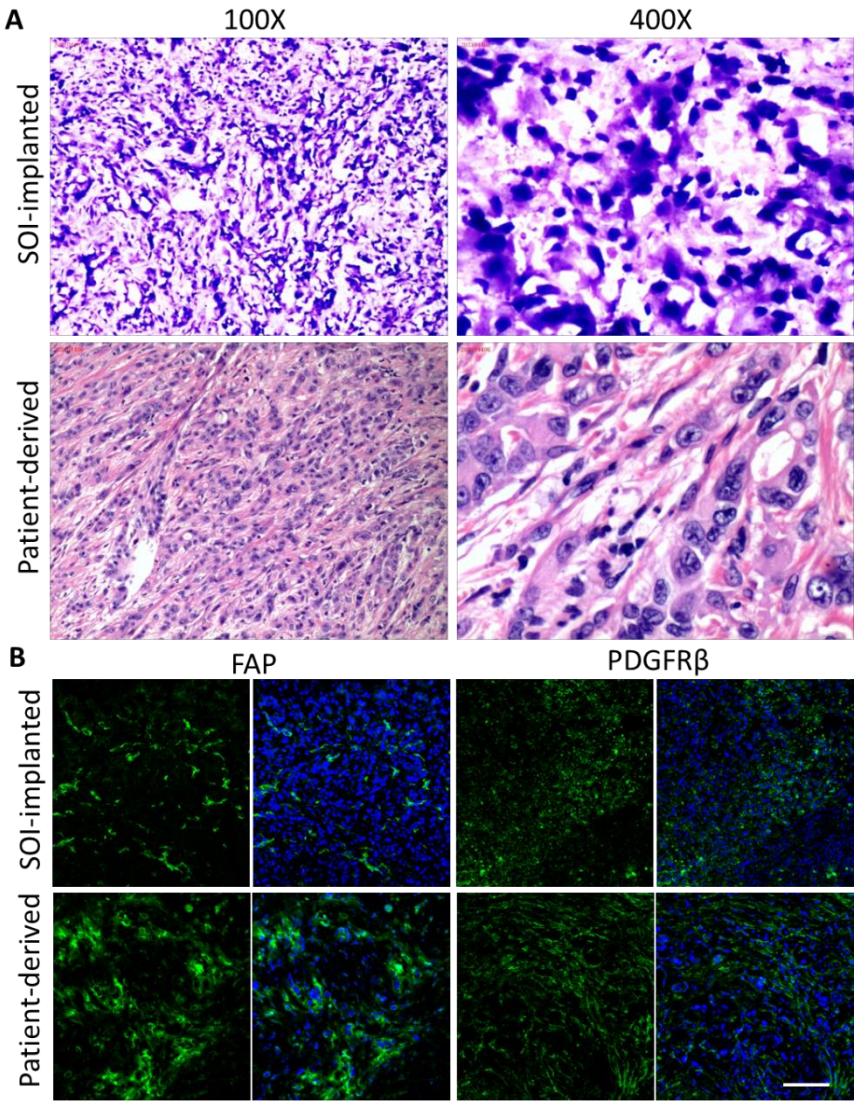

Figure S8. Comparison of the orthotopic PDAC and patient-derived pancreatic cancer tissues. (A) SOI-implanted model showed similar poorly differentiated pancreatic adenocarcinoma structure resembling clinical PDAC, as clarified by a pathologist in Hunan Cancer Hospital. SOI-implanted tumors were prepared in OCT block, whereas the patient-derived cancer tissues were processed in paraffin blocks, which displayed good morphology. (B) Contiguous sections were stained with fibroblast activation protein (FAP) or platelet-derived growth factor receptor β (PDGFR-β) antibody, and nuclei were stained with DAPI (blue), scale bar = 100 μm.

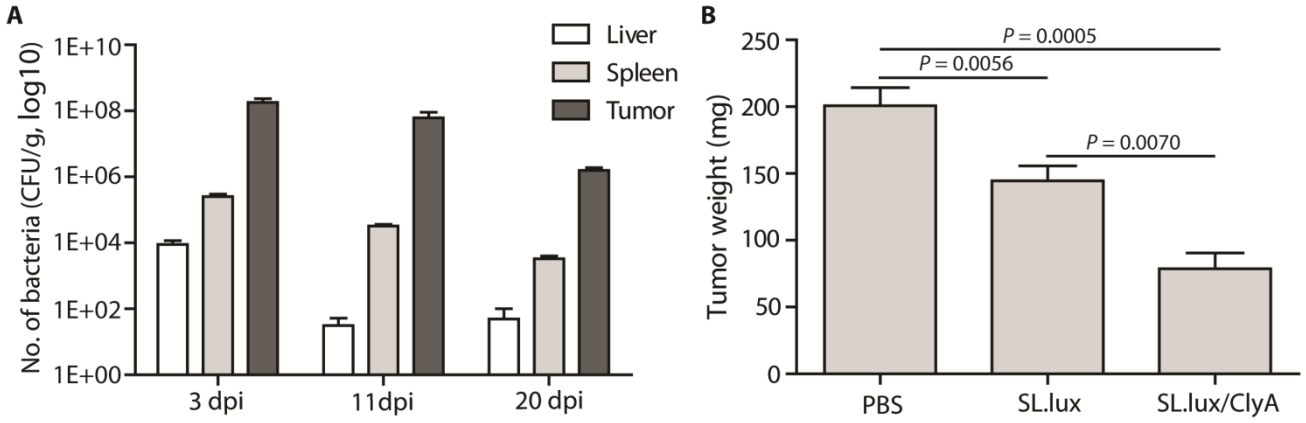

Figure S9. Anticancer activity in the orthotopic pancreatic cancer model. Mice harboring SOI-implanted cancer fragments (AsPC-1/Fluc) were injected intravenously with 3.0×10^7 CFU engineered SL^{lux}, $SL^{lux/ClyA}$, or PBS. (A) Quantification of bacteria in the liver, spleen, and tumor at 3, 11, and 20 days post-bacterial infection (n = 8 mice per group for each time point). (B) Primary tumor weight at Day 22 post-surgical implantation (7 dpi; n = 9 mice per group).

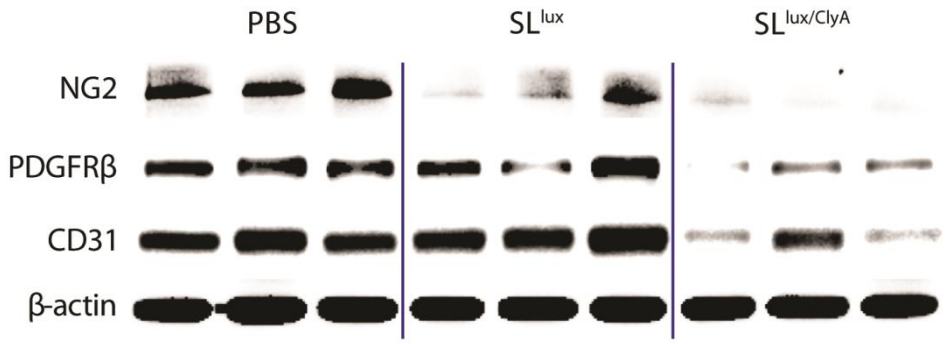

Figure S10. Stromal cell changes after treatment with ClyA-expressing bacteria. Samples were collected at 5 days post-bacterial infection (3.0×10^7 CFU, 48 hours after ClyA induction) from AsPC-1 mice. Expression of stromal cell markers was examined by Western blot analysis. NG2: Neural/glial antigen 2; PDGFRβ: Platelet-derived growth factor receptor β; CD31: Cluster of differentiation 31. Data are representative of at least two independent experiments.

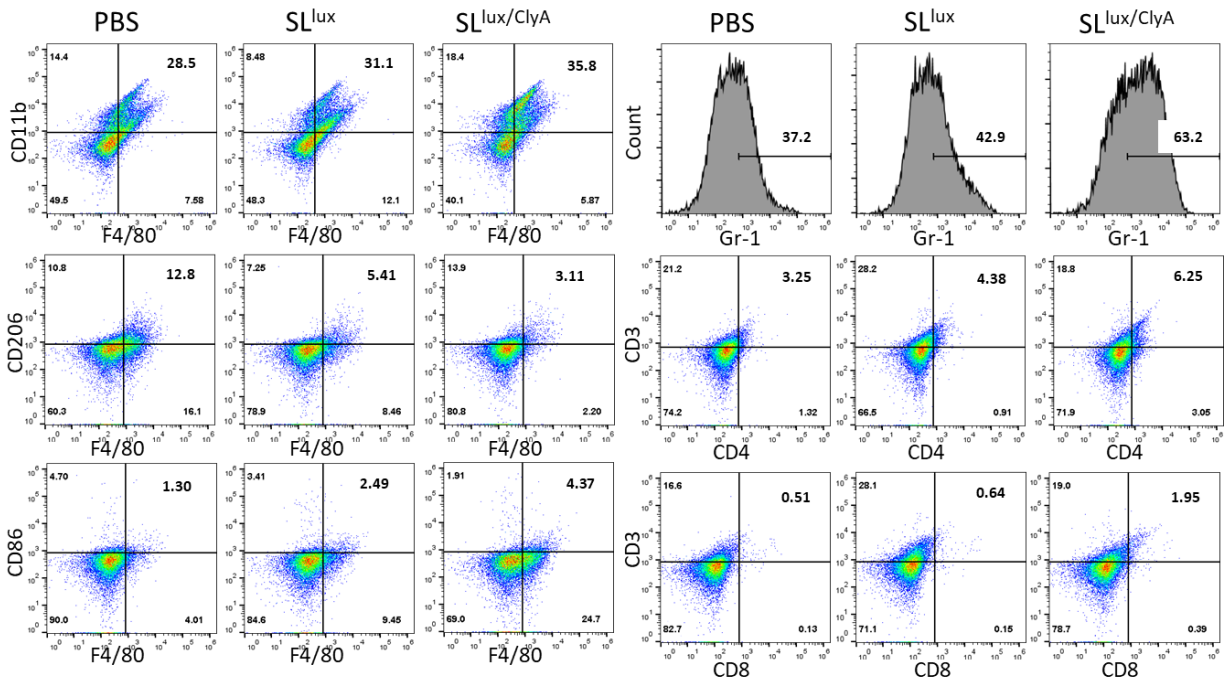

Figure S11. Immune cell analysis in tumor microenvironments. Single-cell suspensions from Pan02 tumors were prepared by incubating removed tumor pieces in 1.0 mg/ml collagenase D (Roche) and 50 µg/ml DNase I (Roche) for 45 min at 37 C, followed by passing through a 40 µm cell strainer. Samples were incubated with specific fluorochrome-labeled antibodies (Table S2) at 4 C for 30 min. At least 20,000 events were analyzed using a FACSCalibur flow cytometer (BD Biosciences). Data were analyzed using FlowJo (TreeStar) software. The analysis gate was set on the basis of isotype plots. Representative data with two independent experiments (n = 3). Macrophage, $CD11b^{+}F4/80^{+}$; M2-type macrophage, $F4/80^{+}$ $CD206^{+}$; M1-type macrophage, $F4/80^{+}$ $CD86^{+}$; Neutrophil, $Gr\text{-}1^{+}$; $CD4^{+}$ T cell, $CD3^{+}CD4^{+}$; $CD8^{+}$ T cell, $CD3^{+}CD8a^{+}$.

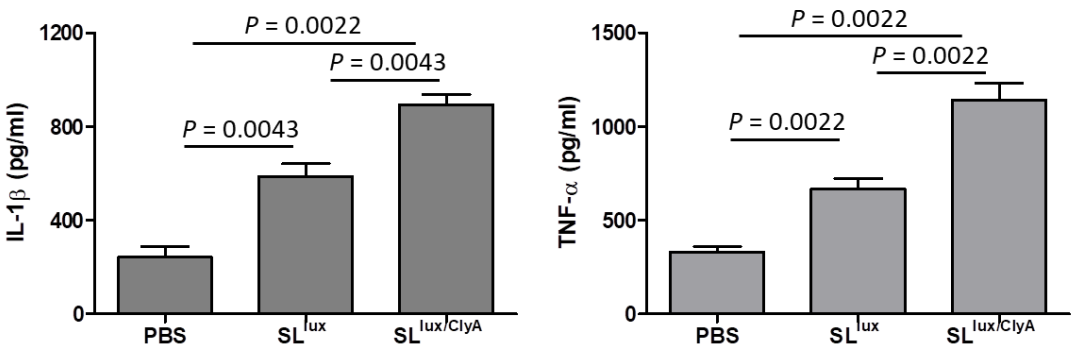

Figure S12. Detection of inflammatory cytokines in tumor tissues. Tumor tissues (n = 6 mice/group) were isolated from Pan02 tumor-bearing mice at 48 h after L-arabinose induction on day 5 post-bacterial infection. Cytokines were detected with IL-1β and TNF-α ELISA kits (eBioscience).

Table S1. Bacterial strains and plasmids used in the study

Strains/plasmids	Relevant genotype	Reference	Injection dose
S. typhimurium ΔppGpp (SL)	Δ*relA*, Δ*spoT*	24	1.0×10^7 CFU/mouse
S. typhimurium ΔppGpp lux (SL^{lux})	Δ*relA*, Δ*spoT*, lux operon	28	3.0×10^7 CFU/mouse
pBAD-Empty	Control vector	15	
pBAD-ClyA	ClyA-encoding	28	

CFU: colony-forming units.

Table S2. Antibodies used in the study

Antibody name	Antibody description	Company/Catalog no.	Remark
Rabbit anti-ClyA polyclonal antibody	Rabbit anti-ClyA	Yeongjin Hong Chonnam National Univ.	**Primary Ab**
Goat anti-*Salmonella* polyclonal antibody	Anti-*Salmonella*	GenWay Biotech/ GWB-AB2632	
β-actin (C4)	Mouse anti-β-actin	Santa Cruz Biotechnology /SC-47778	
Rabbit anti-NG2 chondroitin sulfate proteoglycan	Rabbit anti-NG2	Millipore /AB5320	
Anti-PDGF receptor beta antibody	Rabbit anti-PDGFRβ	Abcam/ab32570	
Anti-CD31 antibody	Rabbit anti-CD31	Abcam/ab28364	
Rat anti-mouse F4/80 (A3-1)	Rat anti-mouse F4/80	AbD Serotec/MCA497GA	
Neutrophil marker (6A608)	Rat mAb anti-mouse neutrophil	Santa Cruz Biotechnology /SC-71674	
Anti-CD4 antibody	Rat mAb anti-mouse CD4	Invitrogen/14-0041	
Anti-CD8a antibody	Rat mAb anti-mouse CD8a	Invitrogen/14-0081	
FAP polyclonal antibody	Rabbit anti-FAP	Invitrogen/PA5-99458	
PDGFRβ monoclonal antibody (G.290.3)	Rabbit anti-PDGFRβ	Invitrogen/MA5-15143	
Peroxidase-conjugated rabbit anti-mouse immunoglobulin	Rabbit anti-mouse	Dako/P0260	**Secondary Ab**
Peroxidase-conjugated goat anti-Armenian hamster immunoglobulin	Goat anti-hamster	Santa Cruz Biotechnology /SC-2443	
Peroxidase-conjugated goat anti-rabbit immunoglobulin	Goat anti-rabbit	Dako/P0448	
Alexa Fluor® 488 donkey anti-rat IgG (H+L) antibody	Donkey anti-rat	Invitrogen/A21208	
Alexa Fluor® 555 donkey anti-rabbit IgG (H+L) antibody	Donkey anti-rabbit	Invitrogen/A31572	
Alexa Fluor® 488 donkey anti-rabbit IgG (H+L) antibody	Donkey anti-rabbit	Invitrogen/A-21206	
Anti-mouse CD45 FITC	mAb (clone 30-F11)	eBioscience/11-0451	**FACS Ab**
Anti-mouse CD11b FITC	mAb (clone M1/70)	eBioscience/11-0112	
Anti-mouse F4/80 antigen PE	mAb (clone BM8)	Biolegend/123110	
Anti-mouse CD3 APC	mAb (clone 17A2)	eBioscience/17-0032	
Anti-mouse CD4 FITC	mAb (clone GK1.5)	eBioscience/11-0041	
Anti-mouse CD8a FITC	mAb (clone 53-6.7)	eBioscience/12-0081	
Anti-mouse Ly-6G (Gr-1) PE	mAb (clone RB6-8C5)	eBioscience/12-5931	
Anti-mouse CD86 (B7-2) APC	mAb (clone GL1)	eBioscience/17-0862	
APC anti-mouse CD206 (MMR)	mAb (clone C068C2)	BioLegend/141708	